第9回地震時保有耐力法に基づく橋梁等構造の
耐震設計に関するシンポジウム講演論文集（2006年2月）

Response Analysis of RC C-bent Columns

Seiji NAGATA[1], Kazuhiko KAWASHIMA[2] and Gakuho WATANABE[3]

[1]Graduate Student, Department of Civil Engineering, Tokyo Institute of Technology, paiboon@cv.titech.ac.jp
[2]Professor, Department of Civil Engineering, Tokyo Institute of Technology, kawasima@cv.titech .ac.jp
[3]Research Associate, Department of Civil Engineering, Tokyo Institute of Technology, gappo@cv.titech .ac.jp
2-12-1 O-okayama Meguro-ku, Tokyo 152-8550

1. INTRODUCTION

In urban areas, peculiar bridges which are supported by C-bent columns have been constructed due to space limitation. Since bending moment and torsion are combined as well as axial force, C-bent columns exhibit complex seismic behavior[1), 2)]. Furthermore extensive residual drift occurs in the eccentric compression side due to the eccentric dead load of the deck during an earthquake.

In this study, an analytical idealization of the torsional hysteresis of C-bent columns is proposed based on a cyclic loading test[1)]. To show the effectiveness of the proposed torsion hysteretic model, an analysis is first conducted assuming that the torsion spring is linear with the initial stiffness for comparison. In addition, a correlation analysis is conducted on the experimental response based on the hybrid loading test[2)]. This paper presents a series of analytical correlations on the experimental response.

2. EXPERIMENTAL RESULTS

(1) Test Specimen and Test Procedure

The columns with the eccentricity being equal to the width of the column D was used in both the cyclic and hybrid loading tests as shown in **Fig. 1**. They were designed in accordance with the Japan seismic design codes[3)] assuming that they were "small prototype" columns. They had a 400mm x 400mm square section with an effective height from the bottom to the loading point of 1350mm.

Although various loading orbits (unilateral and bilateral) were used in the cyclic loading test[1)], the seismic behavior of the columns under unilateral cyclic loading in the longitudinal direction and a constant vertical load is analyzed here. This is because the cyclic loading in the longitudinal direction results in residual drift in the transverse direction as well as complex combined bending and torsion coupling. An axial force was set to be 160kN which induced a 1MPa compression stress at the plastic hinge of the column. Lateral force was

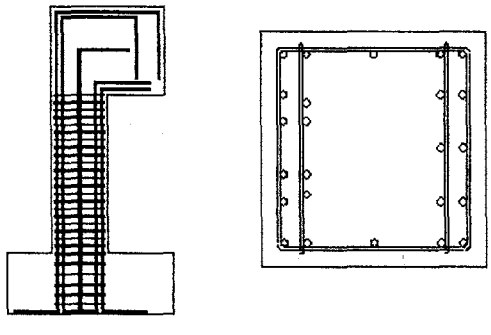

Fig. 1 Test Specimen

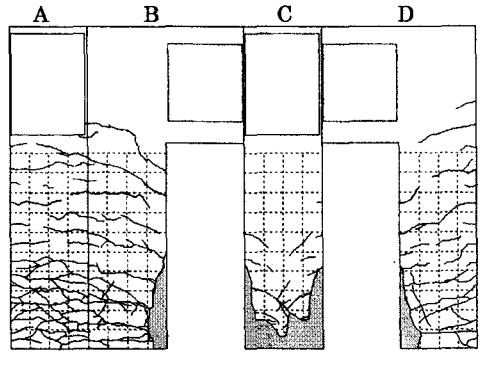

Fig. 2 Failure Mode after the Cyclic Loading[1)]

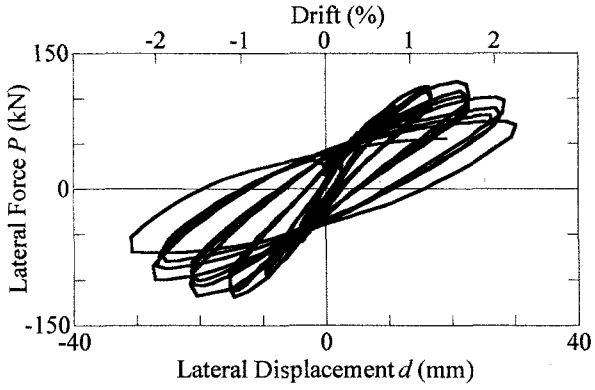

Fig. 3 Lateral Force vs. Lateral Displacement Hysteresis under the Cyclic Loading Test[1)]

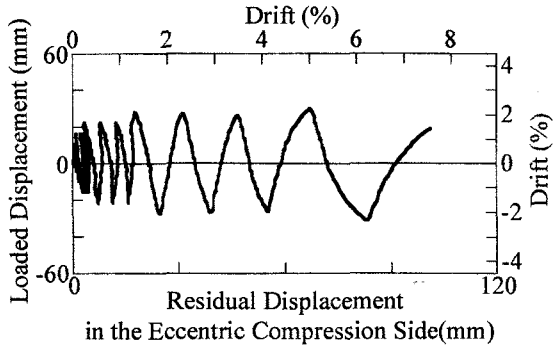

Fig. 4 Residual Displacement due to the Eccentrc Moment under the Cyclic Loading Test[1)]

imposed to the columns under the displacement control. The amplitude of the lateral displacement was step-wisely increased from 0.5% drift until failure with an increment of 0.5% drift. Three cyclic loadings were imposed at each step.

In the hybrid loading test, the column was subjected to the bilateral excitation under a constant vertical load of 160 kN[2)]. The ground acceleration recorded at JMA Kobe Observatory during the 1995 Kobe earthquake was used as an input motion by scaling down its intensity to 30% of the original. NS and EW components were used in the longitudinal and transverse directions, respectively.

(2) Seismic Behavior under the Cyclic Load[1)]

Fig. 2 shows the failure modes of the columns after the 2.5 % drift cyclic loading. Faces A and C are the eccentric tension side and the eccentric compression side, respectively. Damage of the column at the eccentric compression side was much more extensive than the eccentric tension side. Some diagonal cracks were formed due to torsion. It is known that diagonal cracks occur in the columns subjected to combined bending and torsion[4)]. The extensive failure at the eccentric compression side resulted in residual tilt of the columns in the eccentric compression side.

Fig. 3 shows the lateral force and lateral displacement hysteresis of the columns at the loading point. Deterioration of lateral restoring force and displacement ductility capacity are extensive in the C-bent column. The restoring force starts to deteriorate at 2% drift in the column. Torsion resulted in the stiffness degradation in the unloading path. As described earlier, important failure mode of the C-bent column is the residual

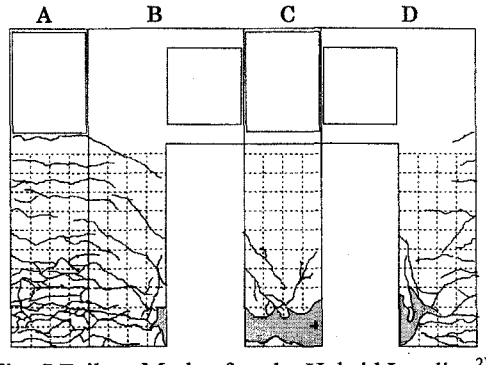

Fig. 5 Failure Mode after the Hybrid Loading[2)]

tilt in the eccentric compression side as shown in **Fig. 4**. For example, the residual drift reached 1.3% drift at 1.5% drift cyclic loading in the column. This must increase the risk of failure of bridges supported by C-bent columns during an earthquake.

(3) Experimental Response under Hybrid Load[2)]

Fig. 5 shows the failure modes of the columns after the hybrid loading. The failure mode after the hybrid loading is quite similar to that under the cyclic loading. Damage of the column at the eccentric compression side was much more extensive than the eccentric tension side. Some diagonal cracks were developed due to torsion.

Figs. 6 and **7** show the displacement response and the lateral force vs. lateral displacement hystereses of the column under the bilateral excitation. The maximum displacement was 3.9 % and 4.6 % drift in the longitudinal and transverse directions, respectively. The residual displacement in the longitudinal direction was not significant, while the large residual displacement corresponding to 4.1 % drift was developed in the eccentric compression side due to the eccentric moment. Based on **Fig. 7**, the lateral strength was 133.6 kN

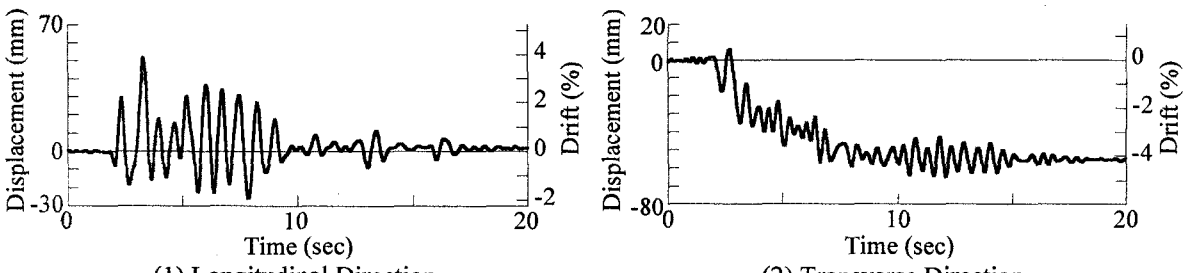

(1) Longitudinal Direction (2) Transverse Direction

Fig. 6 Displacement Response under the Hybrid Loading[2)]

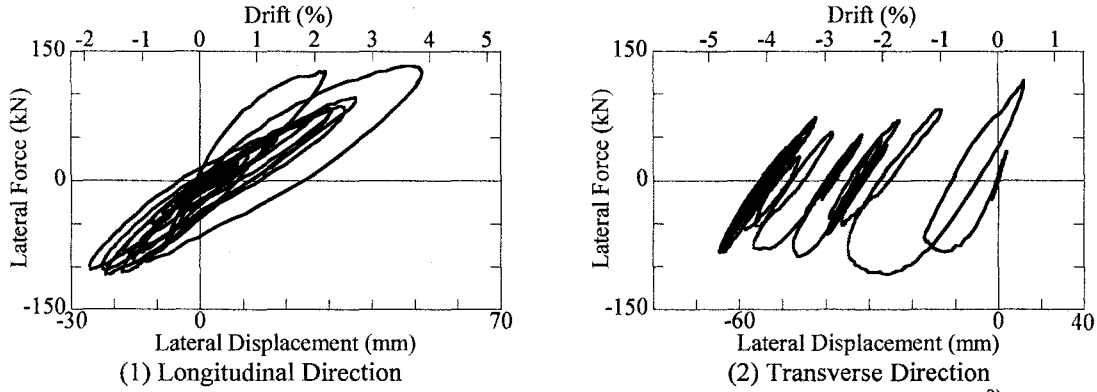

(1) Longitudinal Direction (2) Transverse Direction

Fig. 7 Lateral Force vs. Lateral Displacement Hystereses under the Hybrid Loading[2)]

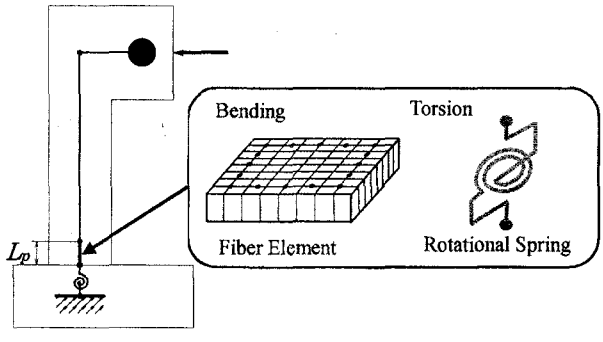

Fig. 8 Idealization of the Test Specimen

and -117 kN in the longitudinal and transverse directions, respectively. Significant deteriorations of the restoring force did not occur in the both columns.

3. ANALYTICAL IDEALIZATION

To correlate the experimental response, the columns are idealized as shown in **Fig. 8**. The plastic flexural deformation of the columns at the plastic hinge region is idealized by a fiber element. The column body other than the plastic hinge is idealized by linear beam elements. A torsion spring is used to represent torsion of the column. The interaction of damage by flexure and torsion is disregarded in this analysis. Because deformation of longitudinal reinforcement inside the footing contributes to develop lateral displacement in the columns, it is represented by a linear rotation spring at the bottom of the columns.

In such an idealization, how to determine the plastic hinge length L_p of the column is important, because it was revealed that the columns subjected to combined bending and torsion suffered damage above the usual plastic hinge zone under pure flexural loading depending on the rotation-drift ratio[4)]. However, such an effect of the interaction was less significant in the experimental results, because the compression failure of concrete took place between the bottom of the column and 200 mm high from the bottom as shown in **Figs. 2** and **5**. Thus the plastic hinge length L_p was assumed to be a half of the column width [3)].

In the fiber element, the stress vs. strain

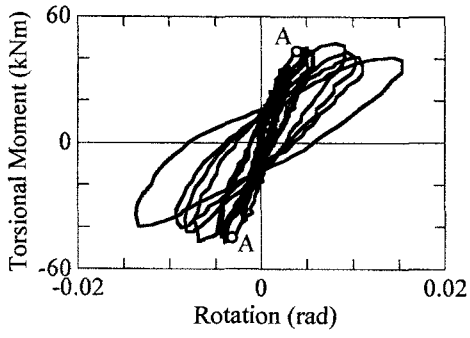

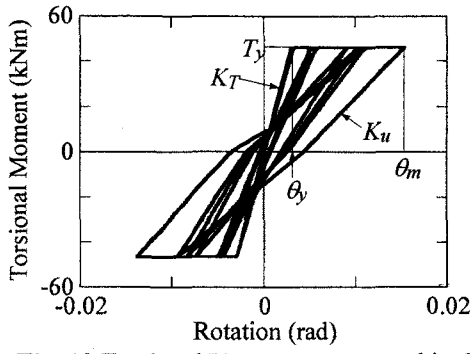

Fig.9 Torsional Hystereses Obtained by the Experiment **Fig. 10** Torsional Hystereses assumed in the Analysis

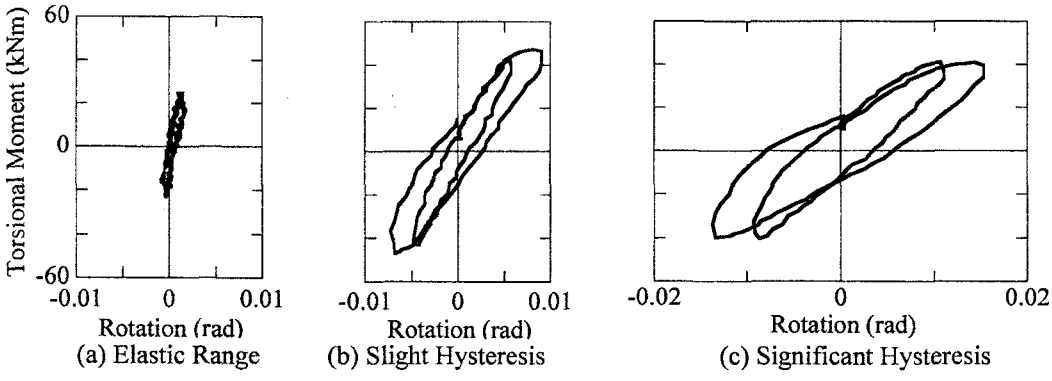

(1) Hysteretic Loops obtained by the Cyclic Loading Test

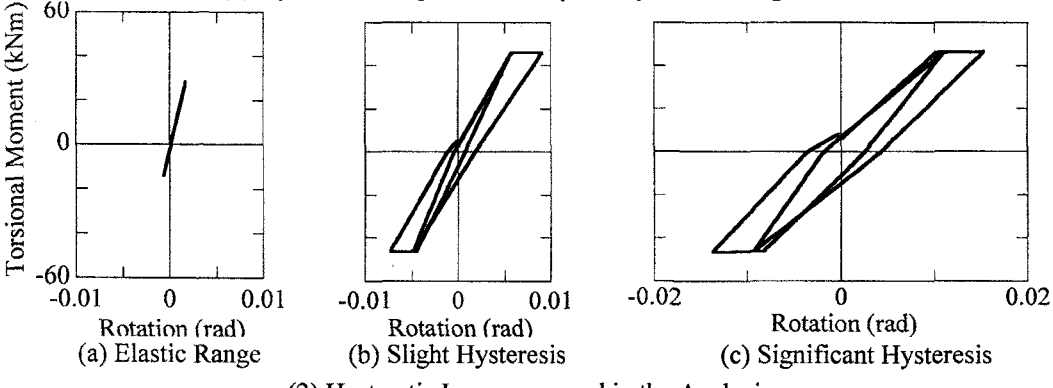

(2) Hysteretic Loops assumed in the Analysis

Fig. 11 Correlation on the Torsional Hysteresis under the Cyclic Loading

relation of confined concrete is idealized by a model by Hoshikuma and Kawashima et al.[5] and unloading and reloading hystereses are idealized based on a model by Sakai and Kawashima[6]. The modified Menegotto-Pinto model [7] · [8] is used to idealize the stress vs. strain relation of the reinforcements.

It is important how to determine the stiffness of the torsion spring. Because torsion of the columns was measured, it is possible to determine the torsion vs. rotation hystereses of the columns at the loading point. **Fig. 9** shows this hysteresis for the column under the cyclic loading. Based on **Fig. 9**, the initial stiffness in the hesteresis is 155.5 MNm/rad, which is corresponding to almost a half of the gross section torsional stiffness (330.0 MNm/rad). The torsional moment starts to yields significantly at point A (0.004 radian). The hysteresis shows that the unloading paths are oriented toward the past largest hysteretic response point. The unloading and reloading stiffness degraded as the rotation increased in the experiment. This is similar to the degrading model proposed by Takeda et al. for flexure[9].

Therefore a bilinear model with the elasto-plastic envelop and the stiffness degrading with the past largest response oriented unloading paths is proposed to represent the torsion spring as shown in **Fig. 10**. The initial stiffness K_T and the unloading stiffness K_u after yield are assumed as

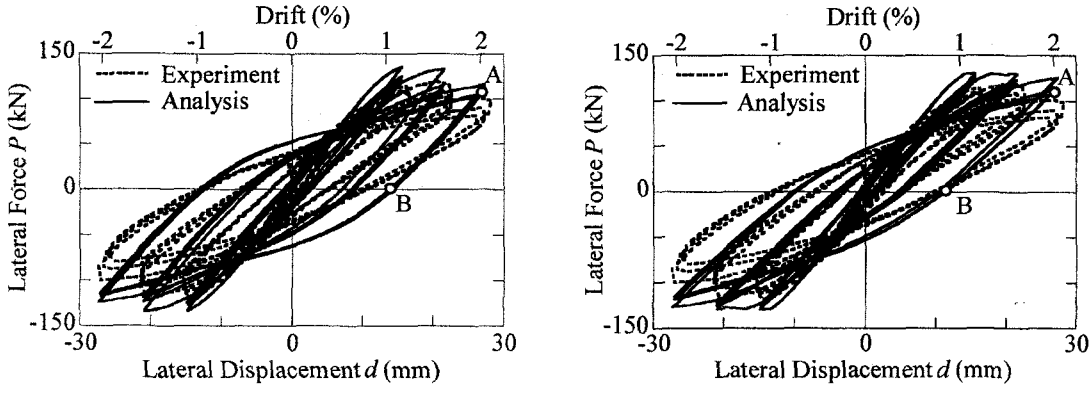

(1) Correlation with the Linear Torsion Spring (2) Correlation with the Nonlinear Torsion Spring

Fig. 12 Correlation on the Lateral Force vs. Lateral Displacement Hysteresis under the Cyclic Loading

$$K_T = \alpha \cdot K_{TG} \quad (1)$$

$$K_u = K_e \left(\theta_y / \theta_m\right)^{\beta} \quad (2)$$

in which K_{TG}: gross section torsional stiffness, θ_y: yield rotation, θ_m: past maximum rotation, α and β are parameters to be determined empirically.

Based on the test results, it is proposed to assume α=0.5 and β=0.8. It is noted that because the initial stiffness presented in **Fig. 9** is no more the full section stiffness but the stiffness with some minor cracks already, α is smaller than 1.0. It is also noted that β which represents the deterioration rate of the unloading stiffness is much larger than the values for flexure[9].

In this analysis the yield rotation θ_y is so determined that maximum rotation θ_m obtained by the experiment is well correlated by the analysis. The yield rotation θ_y in the torsion spring is assumed to be 0.0034 radian and 0.0038 radian, respectively, in the columns under the cyclic and hybrid loadings. The torsion hysteresis predicted by Eqs. (1) and (2) are compared with the test results in **Fig. 11**. It is seen that the empirical hystereses are in good agreement with the test results.

As for the columns without eccentricity, Hayakawa et al. and Ogimoto et al. have conducted the similar analysis without the torsion spring, which showed that the fiber element analysis predicts the test results of the columns without eccentricity with a good accuracy under both unilateral and bilateral loadings[10), 11)]. In the following, to show the effectiveness of the proposed torsion hysteresis on correlation on the column with the eccentricity, an analysis is first conducted assuming that the torsion spring is linear. The effectiveness of the proposed model may be verified by the comparison between the analysis with the linear hysteresis and with the nonlinear hysteresis in the torsion spring.

4. ANALYTICAL CORRELATION

(1) Correlation on the Cyclic Loading Test

Fig. 12 shows the correlation on lateral force vs. lateral displacement hystereses. The linear and nonlinear simulation for the torsion spring is presented here for comparison, as well as the test result. Since torsion resulted in the stiffness degradation in the unloading path, a main concern of the comparison is the correlation of a loading path denoted as A-B. Although the general shape of the hystereses look similar, it is obvious that the proposed hysteretic model provides more realistic behavior than the linear spring model, comparing the unloading path denoted as A-B in **Fig. 12**.

The torsion vs. rotation relation presented in **Fig. 11** can be represented in terms of the lateral force P vs. lateral displacement of the column due to rotation d_r as shown in **Fig. 13**. It is apparent that the linear spring model does not represent the experimental results, while the proposed hysteretic model captures the experimental result.

Fig. 14 shows the correlation on the residual displacement of the column in the eccentric compression side. The nonlinear analysis for the torsion spring is presented here as well as the test result. Based on the correlation, general trend of the residual displacement obtained by the experiment is expressed by the analysis with the proposed model.

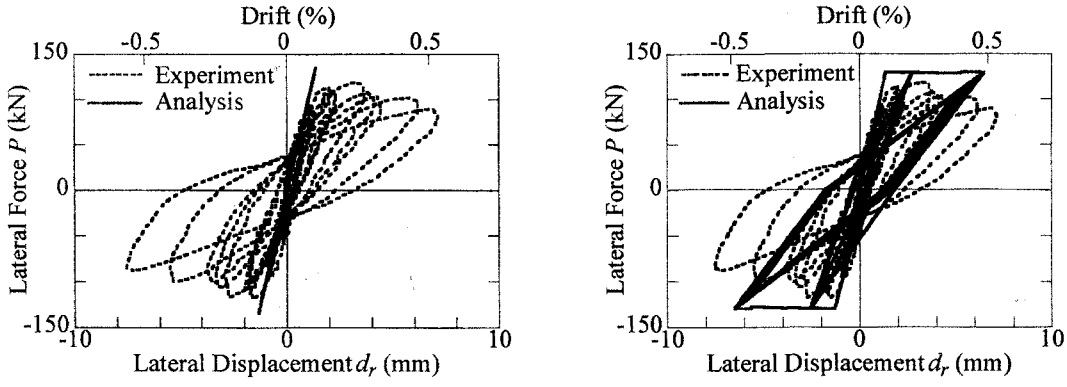

(1) Correlation with the Linear Torsion Spring (2) Correlation with the Nonlinear Torsion Spring

Fig. 13 Correlation on the Lateral Force P vs. Lateral Displacement Hysteresis due to Torsion d_r

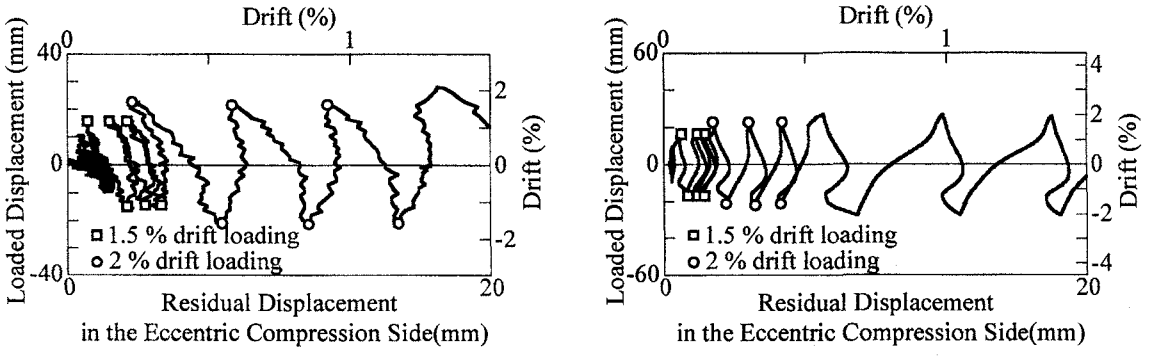

(1) Experimental Result (2) Correlation with the Nonlinear Torsion Spring

Fig. 14 Correlation on the Residual Displacement under the Cyclic Loading

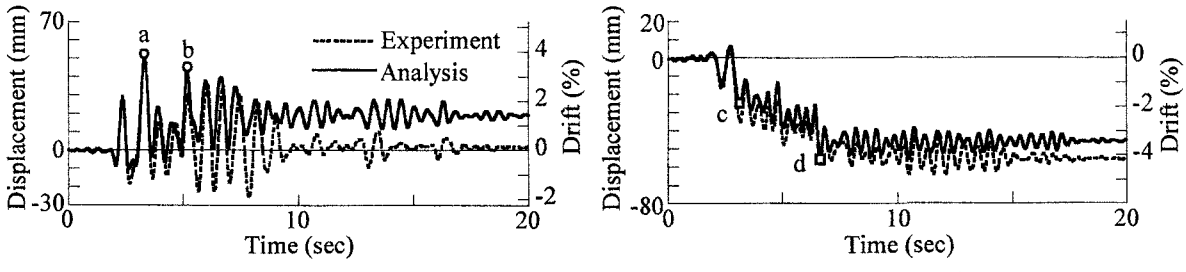

(1) Longitudinal Direction (2) Transverse Direction

Fig. 15 Displacement Response under the Bilateral Seismic Excitation

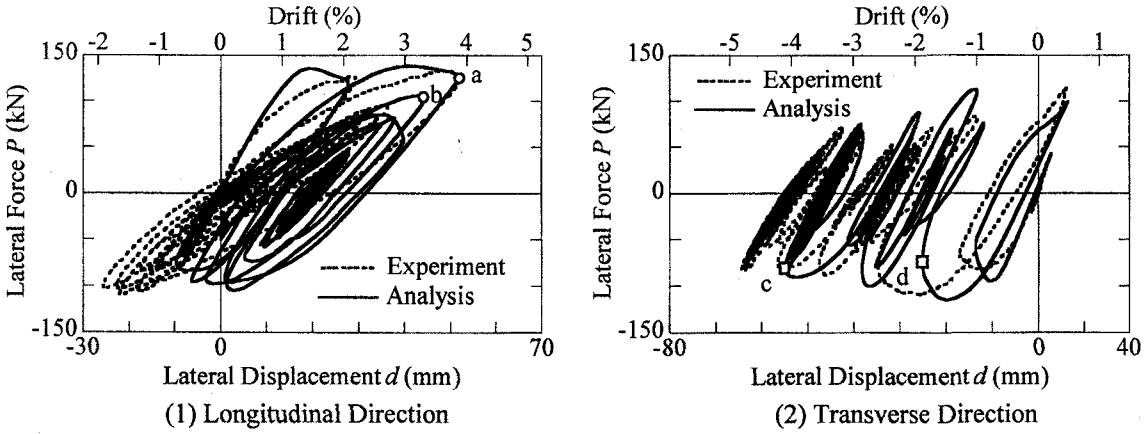

(1) Longitudinal Direction (2) Transverse Direction

Fig. 16 Correlation on the Lateral Force vs. Lateral Displacement Hysteresis under the Bilateral Excitation

(2) Correlation on the Hybrid Loading Test

Fig. 15 compares the analytical result to test result on the displacement response of the column under the bilateral excitation. Correlation on the lateral force vs. lateral displacement hystereses is shown in **Fig. 16**. The overall responses and

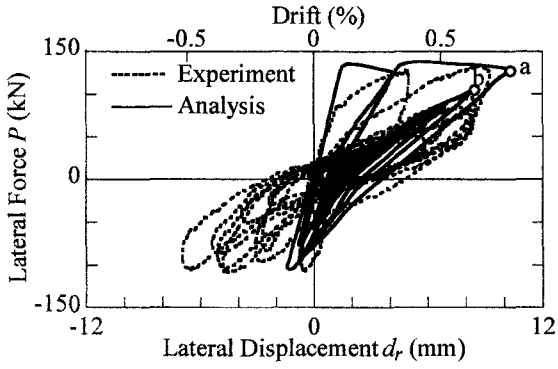

Fig. 17 Correlation on the Lateral Force P vs. Lateral Displacement Hysteresis due to Torsion d_r

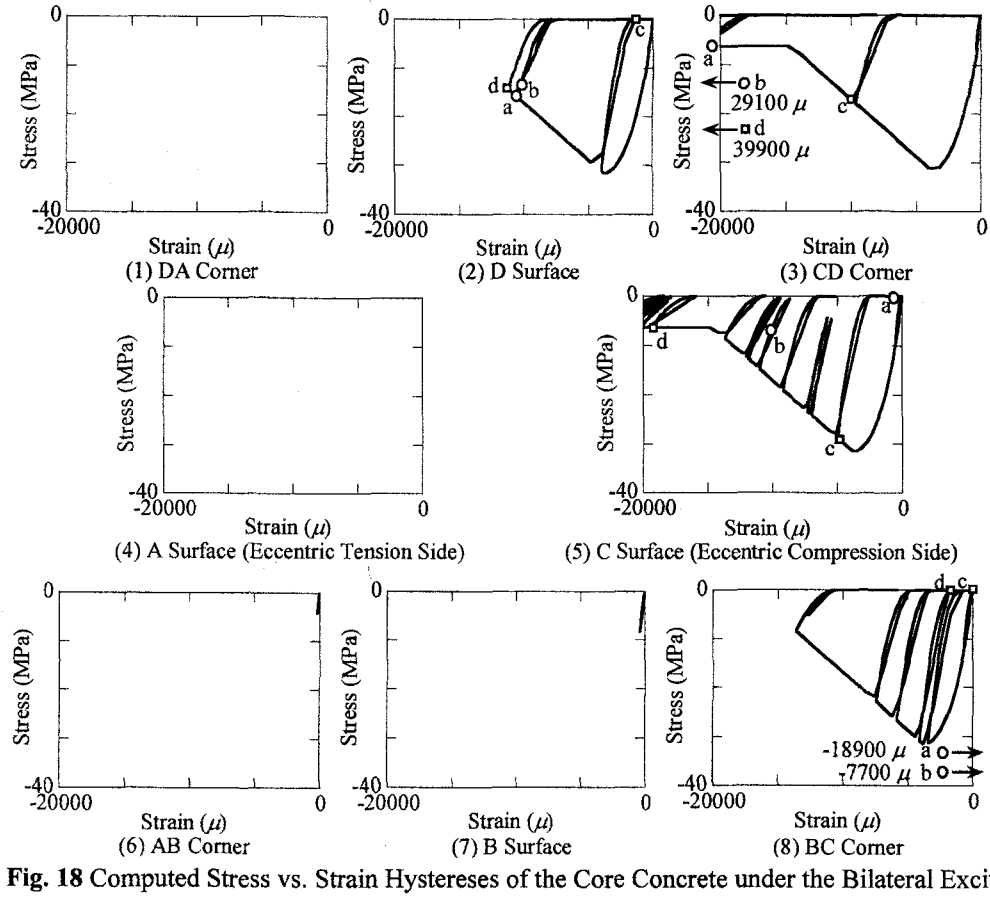

Fig. 18 Computed Stress vs. Strain Hystereses of the Core Concrete under the Bilateral Excitation

hystereses are well simulated by the analysis with the proposed torsion hysteresis including the accumulation of the residual displacement in the eccentric compression direction. In particular, the agreement between the analysis and the experiment is satisfactory until the response started to decay after the peak. **Fig. 17** shows the lateral force P vs. lateral displacement of the column due to rotation d_r the loading point of the columns. The analysis simulates the experimental hysteresis with good accuracy in the column with the eccentricity.

The computed stress vs. strain relations of the core concrete in the column are shown in **Fig. 18**. In the experiment, compression failure of concrete was more extensive in the C and D surfaces and CD corner in the failure mode of the column shown in **Fig. 5**. On the other hand, progress of the strain of the core concrete is more significant at C and D surfaces as well as CD corner than the other sides in the analysis. The failure mode of the columns can be well expressed based on the stress-strain relations obtained by the fiber element analysis.

5. CONCLUSIONS

To correlate the experimental response of C-bent columns, an analytical idealization using a fiber element and a nonlinear torsion spring was proposed. To use the proposed model, a series of correlation analysis using the proposed idealization was conducted on the cyclic and hybrid loading test. The following conclusions may be derived from the results presented herein.

(1) Combined bending and torsion hysteresis of the columns under a seismic excitation have to be idealized properly to have a realistic correlation on the complex experimental behavior of the reinforced concrete C-bent column models.

(2) A model with an elastoplastic bilinear envelop and the stiffness degradation with the past largest response oriented unloading paths was proposed to idealize the torsion spring which represents the combined torsion response of the C-bent columns.

(3) The analysis using the proposed torsion spring represents more realistic behavior under the cyclic loading than the analysis using the linear torsion spring. In particular, comparing an unloading path of the lateral force vs. lateral displacement hystereses, the proposed torsion hysteresis provides more realistic behavior.

(4) Based on the correlation analysis on the hybrid loading test, the analysis simulates well the general trend of the experimental response including the residual drift in the eccentric compression side due to the eccentricity.

REFERENCES

1) Kawashima, K., Watanabe, G., Hatada, S. and Hayakawa, R.: Seismic Performance of C-bent Columns based on a Cyclic Loading Test, *J. Structural Mechanics and Earthquake Engineering*, JSCE, No. 745/I-65, pp. 171-189, 2003.

2) Nagata, S., Kawashima, K. and Watanabe, G.: Seismic Response of RC C-bent Columns based on a Hybrid Loading Test, *Proc. 1st International Symposium on Advances in Experimental Structural Engineering*, pp. 227-234, Nagoya, Japan, 2005.

3) Japan Road Association: *Part V seismic design, design specifications of highway bridges*, Maruzen, Tokyo, Japan, 2002.

4) For example, Tirasit, P. and Kawashima, K.: Combined Cyclic Bending-Torsional Loading Test of Reinforced Concrete Bridge Columns, *21st US-Japan Bridge Engineering Workshop*, PWRI, Tsukuba, Japan, 14 pases, 2005.

5) Hoshikuma, J., Kawashima, K., Nagaya, K. and Taylor, A. W.: Stress-Strain Model for Confined Reinforced Concrete in Bridge Piers, *J. Structural Engineering*, ASCE, 123(5), pp. 624-633.1997.

6) Sakai, J. and Kawashima, K.: An Unloading and Reloading Stress-Strain Model for Concrete confined by Tie Reinforcements, *Proc.12th World Conference of Earthquake Engineering*, No. 1432 (CD-ROM), Auckland, New Zealand, 2000.

7) Menegotto, M. and Pinto, P.E.: Method of Analysis for Cyclically Loaded R.C. Plane Frames including Changes in Geometry and Non-Elastic Behavior of Elements under Combined Normal Force and Bending, *Proc. IABSE Symposium on Resistance and Ultimate Deformability of Structures Acted on by Well Defined Repeated Loads*, pp. 15-22, 1973.

8) Sakai, J. and Kawashima, K.: Modification of the Giuffre, Menegotto and Pint Model for Unloading and Reloading Paths with Small Strain Variations, *J. Structural Mechanics and Earthquake Engineering*, JSCE, No. 738/I-64, 159-169, 2003.

9) Takeda, T., Sozen, A., and Nielsen, N.: Reinforced Concrete Response to Simulated Earthquakes, *J. Structural Division*, ASCE, Vol. 96, ST12, pp. 2557-2573, 1970.

10) Hayakawa, R., Kawashima, K., and Watanabe, G: Effect of Bilateral Loadings on the Flexural Strength and Ductility Capacity of Reinforced Concrete Bridge Column, *J. Structural Mechanics and Earthquake Engineering*, JSCE, No. 759/I-67, pp. 79-98, 2004.

11) Ogimoto, H., Kawashima, K., Watanabe, G., and Nagata, S.: Effect of Bilateral Excitation on the Seismic Performance Reinforced Concrete Bridge Columns based on a Hybrid Loading Test, *J. Structural Mechanics and Earthquake Engineering*, JSCE, No. 801/I-73 pp. 33-50, 2005.